Virologica Sinica 38 (2023) 387–397

Contents lists available at ScienceDirect

Virologica Sinica

journal homepage: www.keaipublishing.com/en/journals/virologica-sinica
www.virosin.org

Research Article

3C^{pro} of FMDV inhibits type II interferon-stimulated JAK-STAT signaling pathway by blocking STAT1 nuclear translocation

Xiangju Wu [a,1], Lei Chen [b,1], Chao Sui [a], Yue Hu [a], Dandan Jiang [a], Fan Yang [c], Laura C. Miller [d], Juntong Li [a], Xiaoyan Cong [a], Nataliia Hrabchenko [a], Changhee Lee [e], Yijun Du [a,b,*], Jing Qi [a,b,*]

[a] Shandong Key Laboratory of Animal Disease Control and Breeding/Key Laboratory of Livestock and Poultry Multi-omics of MARA, Institute of Animal Science and Veterinary Medicine, Institute of Crop Germplasm Resources, Shandong Academy of Agricultural Sciences, Jinan, 250100, China
[b] College of Life Science, Shandong Normal University, Jinan, 250358, China
[c] State Key Laboratory of Veterinary Etiological Biology/National Foot and Mouth Disease Reference Laboratory/Key Laboratory of Animal Virology of Ministry of Agriculture, Lanzhou Veterinary Research Institute, Chinese Academy of Agricultural Sciences, Lanzhou, 730050, China
[d] Department of Diagnostic Medicine and Pathobiology, College of Veterinary Medicine, Kansas State University, Manhattan, KS, 66506, USA
[e] College of Veterinary Medicine and Virus Vaccine Research Center, Gyeongsang National University, Jinju, 52828, Republic of Korea

ARTICLE INFO

Keywords:
Foot-and-mouth disease virus (FMDV)
3C
IFN-γ
JAK-STAT signaling pathway
STAT1
KPNA1

ABSTRACT

Foot-and-mouth disease virus (FMDV) has developed various strategies to antagonize the host innate immunity. FMDV L^{pro} and 3C^{pro} interfere with type I IFNs through different mechanisms. The structural protein VP3 of FMDV degrades Janus kinase 1 to suppress IFN-γ signaling transduction. Whether non-structural proteins of FMDV are involved in restraining type II IFN signaling pathways is unknown. In this study, it was shown that FMDV replication was resistant to IFN-γ treatment after the infection was established and FMDV inhibited type II IFN induced expression of IFN-γ-stimulated genes (ISGs). We also showed for the first time that FMDV non-structural protein 3C antagonized IFN-γ-stimulated JAK-STAT signaling pathway by blocking STAT1 nuclear translocation. 3C^{pro} expression significantly reduced the ISGs transcript levels and palindromic gamma-activated sequences (GAS) promoter activity, without affecting the protein level, tyrosine phosphorylation, and homodimerization of STAT1. Finally, we provided evidence that 3C protease activity played an essential role in degrading KPNA1 and thus inhibited ISGs mRNA and GAS promoter activities. Our results reveal a novel mechanism by which an FMDV non-structural protein antagonizes host type II IFN signaling.

1. Introduction

Foot-and-mouth disease (FMD) is an acute, highly contagious viral disease caused by FMD virus (FMDV). FMDV can infect cattle, sheep, pigs, and other numerous cloven-hoofed animals and is characterized by acute and long-term, asymptomatic but persistent infection (Stenfeldt et al., 2016). FMDV has a positive-sense, single-stranded RNA and belongs to the genus *Aphthovirus* of the family *Picornaviridae* (Grubman and Baxt, 2004; Jamal and Belsham, 2018). The genome of FMDV contains a single open reading frame (ORF) of approximately 7 kb (Grubman, 1980). The ORF is translated as a polypeptide precursor into a polyprotein of approximately 250 kDa, and then mainly cleaved by two viral proteases [leader (L^{pro}) and 3C^{pro}] to produce structural and non-structural proteins (Robertson et al., 1985).

Interferons (IFNs) are a group of widely expressed cytokines with potent antiviral activity. It can be divided into three categories: type I, type II and type III IFNs (Ikeda et al., 2002; Dunn et al., 2005; Dunn et al., 2006; Kotenko, 2011). There are over 20 members in type I IFN, while there is only one member in type II IFN, IFN-γ (Schoenborn and Wilson, 2007). The *IFN-γ* gene is sited on chromosome 10 in mice and chromosome 12 in humans, respectively. IFN-γ is predominantly produced by mitogenically activated T cells and natural killer (NK) cells during immune response (Randall and Goodbourn, 2008). After secretion, IFN-γ binds to the IFN-γ receptor (IFNGR) which consists of two IFNGR1 and two IFNGR2. As bound by IFN-γ, heterotetrameric IFNGR1/2 subunits heterotetramerize and activate Janus associated kinases (JAKs) (Lasfar et al., 2014). Activated JAKs recruit and phosphorylate the STATs. STAT1 is the main downstream effector of IFN-γ among the STAT family members. Upon

* Corresponding authors.
E-mail addresses: duyijun0916@163.com (Y. Du), qj-happy2008@163.com (J. Qi).
[1] Xiangju Wu and Lei Chen contributed equally to this work.

https://doi.org/10.1016/j.virs.2023.03.003
Received 26 October 2022; Accepted 8 March 2023
Available online 14 March 2023

activated by JAKs, STAT1 homodimerizes and translocates to the nucleus via interaction with a specific nuclear localization signal receptor, karyopherin α1 (KPNA1) (Platanias, 2005; Fros et al., 2010). The STAT1 homodimer then binds to gamma-activated sequences (GAS) promoter of certain IFN-γ-stimulated genes (ISGs), and initiates the transcription of these ISGs (Platanias, 2005; Lang et al., 2012; Kulkarni et al., 2016).

FMDV has developed strategies to counteract host innate antiviral response. L^{pro} and $3C^{pro}$ are proved to antagonize type I IFN immunity. L^{pro} reduces the level of immediately early IFN-β mRNA induction and multiple interferon regulatory factor (IRF) responsive genes, such as *2′, 5′-OAS*, *ISG54*, *IP-10* and *RANTES* in swine cells (De Los Santos et al., 2006). Furthermore, L^{pro} degrades p65/RelA subunit of NF-κB and IRF-3/7, both of which play significant roles in type I IFN production (De Los Santos et al., 2006; Wang et al., 2010). $3C^{pro}$ has been demonstrated to cleave NF-κB essential modulator (NEMO), and therefore suppress NEMO activating IFN production and participating in the RIG-I/MDA5 pathway (Wang et al., 2012). $3C^{pro}$ degraded PRDX6 through its proteolytic activity to antagonize host antiviral response (Wang et al., 2021). Previously, we have found that $3C^{pro}$ could antagonize IFN-β signaling pathway through blocking the nuclear translocation of STAT1/STAT2 (Du et al., 2014). For FMDV proteins that counteract the type II IFN signaling pathways, it has been reported that FMDV structural protein VP3 degrades Janus kinase 1 and suppresses STAT1 phosphorylation, dimerization and nuclear accumulation (Li et al., 2016). However, whether FMDV non-structural proteins involve in inhibiting type II IFN signaling pathways remains unknown.

In this study, we aimed to investigate the function of FMDV non-structural protein 3C in type II IFN signaling pathway. First, we analyzed FMDV titers and ISGs induction in PK-15 cells pretreated with IFN-γ prior to or after FMDV infection. It was found that FMDV interfered with type II IFN signaling pathway. Furthermore, our results indicate that FMDV non-structural protein 3C antagonizes type II IFN-stimulated JAK-STAT signaling pathway through blocking STAT1 nuclear translocation. With the protease activity of $3C^{pro}$ degrading KPNA1, FMDV $3C^{pro}$ not only antagonizes the type I IFN signaling pathway (Du et al., 2014), but also inhibits the type II IFN signaling pathway, suggesting an essential role of $3C^{pro}$ in FMDV counteracting the host innate immune response and facilitating FMDV replication in host cells.

2. Materials and methods

2.1. Cells and chemicals

Porcine kidney (PK-15), BHK-21 and HeLa cells were cultured in Dulbecco's modified Eagle's Medium (Fisher Scientific, Waltham, MA, USA) supplemented with 10% fetal bovine serum (FBS; HyClone, Logan, UT, USA), 2 mmol/L L-glutamine, 100 U penicillin/mL and 100 μg streptomycin/mL in a humidified incubator with 5% CO_2 at 37 °C. Porcine IFN-γ (R&D Systems, Minneapolis, Minnesota, USA) and human IFN-γ (Calbiochem, San Diego, CA, USA) were used for IFN stimulation in PK-15 and HeLa cells, respectively.

2.2. Plasmids

The plasmid pGAS-Luc contains the GAS binding sequence upstream of the luciferase reporter gene (Stratagene, La Jolla, CA, USA). The pRL-TK plasmid (Promega, Madison, WI, USA) contains the *Renilla* luciferase reporter, serving as an internal control. pXJ41-3ABC (FLAG and HA tags), pXJ41-3A (FLAG tag), pXJ41-3B (FLAG tag), pXJ41-3C (HA tag), pXJ41-3C site-specific mutations (H46Y, D84N, C163G, and H205R), and pXJ41-GST were described previously (Du et al., 2014). *KPNA1* gene was amplified from the cDNA of HeLa cells with primers KPNA1-Fwd and KPNA1-Rev fused with an N-terminal FLAG tag (Du et al., 2014) and cloned into pXJ41 vector to obtain pXJ41-FLAG-KPNA1. All of these plasmids were sequenced and accorded with the correct tandem in-frame insertion of individual genes.

2.3. Virus titers determination

To investigate whether FMDV interferes with type II IFN, PK-15 cells were seeded in two 24-well plates. With cells reaching approximately 70%–80% confluence, one plate of PK-15 cells were separately pretreated with 0, 50, 100, 200, 400 ng/mL porcine IFN-γ for 5 h and then infected with FMDV O/BY/CHA/2010 (GenBank accession no. JN998085) at an MOI of 0.1 for another 24 h. The other plate of PK-15 cells were infected with FMDV O/BY/CHA/2010 at an MOI of 0.1 for 24 h before treated with 0, 50, 100, 200, 400 ng/mL porcine IFN-γ for 5 h. Cells were frozen-thawed twice and the 50% tissue culture infective dose ($TCID_{50}$) was measured on BHK-21 cells. In brief, BHK-21 cells were cultured in 96-well plate and grew to 70%–80% confluence. Samples were diluted by DMEM containing 2% fetal bovine serum from 10^{-1} to 10^{-10} continuously. Each diluted sample was inoculated into eight replicates of BHK-21 cell monolayer. CPE in each well was observed microscopically for 4 days and $TCID_{50}$ was determined by the Reed and Muench method (Pizzi, 1950).

2.4. Analysis of ISGs mRNA

The mRNA levels of porcine ISGs (GBP2, ISG15, ISG56, OAS and PKR) or human ISGs (GBP1, ISG15, ISG56, OAS and PKR) were detected by real-time PCR. PK-15 cells were inoculated with FMDV or UV-inactivated FMDV at an MOI of 0.1 for 24 h before treated with porcine IFN-γ (200 ng/mL) for 5 h. After being transfected with indicated plasmids, HeLa cells were stimulated with human IFN-γ (100 ng/mL) for 5 h at 24 h post-transfection. Total RNA was extracted from PK-15 or HeLa cells by using TRIzol reagent (Invitrogen, Carlsbad, CA, USA) according to the manufacturer's regulations. RNA was further purified using RNeasy Mini kit (Qiagen, Chatsworth, CA, USA). Approximately 1 μg of purified RNA was used to synthesize cDNA with oligo (dT) primer and SuperScript™ III Reverse Transcriptase (Invitrogen, Carlsbad, CA, USA), and then 1 μL cDNA was used as a template for SYBR green PCR assay (Applied Biosystems). Primers in this study are shown in Supplementary Table S1. For each sample, the mRNA level was measured three times and normalized to that of porcine or human GAPDH mRNA. Relative transcript levels quantified by the $2^{-\Delta\Delta Ct}$ (threshold cycle) method were shown as relative fold changes in comparison with the mock-treated control level of untransfected cells.

2.5. Luciferase reporter gene assay

HeLa cells growing to 70%–80% confluence in 12-well plates were transfected with indicated plasmids and 0.5 μg of pGAS-Luc as well as 0.05 μg of pRL-TK using Lipofectamine™ 3000. After 24 h transfection, cells were treated with 100 ng/mL of human IFN-γ. 16 h later, cells were harvested for luciferase activity measure using the dual-luciferase reporter assay system (Promega, Madison, WI, USA) as described previously (Du et al., 2014).

2.6. Western blot analysis assay

HeLa or PK-15 cells were lysed in the precooled lysis buffer added with phenylmethylsulfonyl fluoride (PMSF; Beyotime, China). The samples were resolved in a 12% sodium dodecyl sulfate-polyacrylamide gel. Separated proteins were then transferred onto a nitrocellulose membrane and incubated with antibody against STAT1 (Cell Signaling, Danvers, MA, USA), phospho-STAT1 (Tyr701, herein named STAT1-Y701, Cell Signaling), FLAG (Sigma-Aldrich, St. Louis, MO, USA), HA (Sigma-Aldrich), heat shock protein 90 (HSP90; Santa Cruz Biotechnology, Santa Cruz, CA, USA), poly (ADP-ribose) polymerase (PARP; Santa Cruz Biotechnology), rabbit anti-3C serum (kept in our laboratory) or β-actin antibody (Santa Cruz Biotechnology), respectively. The membranes were then incubated with HRP-conjugated affinipure goat anti-rabbit IgG or goat anti-mouse IgG (Boster, Wuhan, China), respectively. The membranes were then developed using WesternBright™ Sirius detection kit on the basis of the manufacturer's instructions (Advansta, Menlo Park,

CA, USA). Digital signal was acquired and analyzed by the Quantity One program, version 4.6 (Bio-Rad).

2.7. Dimerization assay

HeLa cells seeded in 6-well plates were transfected with pXJ41 or pXJ41-3C for 24 h. Then 100 ng/mL of human IFN-γ was added and 1 h later, cells were harvested and analyzed by native-PAGE or SDS-PAGE as described previously (Mori et al., 2004). The STAT1 monomer and dimer were detected by native-PAGE and immunoblotting with antibody against STAT1. The expression of 3C and β-actin were detected by SDS-PAGE and immunoblotting with antibody against HA or β-actin.

2.8. Indirect immunofluorescence assay (IFA)

HeLa cells seeded on coverslips were transfected with plasmid pXJ41, pXJ41-3C, or individual mutants of pXJ41-3C. After 18 h transfection, 100 ng/mL of human IFN-γ was added to cells for 1 h. Then cells were washed twice in ice-cold phosphate-buffered saline (PBS) and fixed with 4% paraformaldehyde at 4 °C for 1 h. Cells were then washed three times and permeabilized with 0.5% Triton X-100 for 15 min. The coverslips were then incubated with anti-STAT1 polyclonal Ab (1:1000) and anti-HA antibody (MAb; 1:800) in PBS for 1 h. After three PBS washes, coverslips were incubated with Alexa Fluor 488-conjugated goat anti-mouse IgG (H+L) and Alexa Fluor 594-conjugated goat anti-rabbit IgG (H+L) antibodies at room temperature for 1 h. Then the coverslips were washed three times and treated with DAPI (4′,6′-diamidino-2-phenylindole) (Sigma-Aldrich) to view the nuclei, followed by five washes. The coverslips were then mounted with mounting buffer (60% glycerol and 0.1% sodium azide in PBS) and observed under Confocal Laser Scanning Microscope SP8 (Leica).

2.9. Subcellular fractionation

HeLa cells were transfected with pXJ41 and pXJ41-3C or its individual mutants for 18 h and then treated with 100 ng/mL human IFN-γ for 1 h. Cells were washed in PBS and centrifugated at 4 °C for 5 min. Nuclear and cytosolic fractions were extracted according to the manufacturer's suggestions using a nuclear/cytosol fractionation kit (BioVision; Mountain View, CA, USA) as described previously (Du et al., 2014). Western blotting was performed for further analysis of these cytoplasmic and nuclear extracts. β-actin, HSP90 and PARP antibodies were used to estimate the result of fractionation.

2.10. Statistical analysis

All assays were repeated three times, and data represent the mean ± the standard deviations (SD) of three independent experiments. Statistical differences between groups were determined by one-way analysis of variance (ANOVA) and least significance difference (LSD). A *P*-value <0.05 was considered statistically significant (Wu et al., 2018).

3. Results

3.1. FMDV interferes with type II IFN induction of ISGs expression in PK-15 cells

To investigate whether FMDV interferes with type II IFN, PK-15 cells were separately pretreated with 0, 50, 100, 200, 400 ng/mL porcine IFN-γ for 5 h prior to FMDV infection. As seen in Fig. 1A, FMDV titers were decreased in a concentration-dependent manner, indicating that IFN-γ had anti-FMDV activity before FMDV infection. However, when PK-15 cells were infected with FMDV and treated with 0, 50, 100, 200, 400 ng/

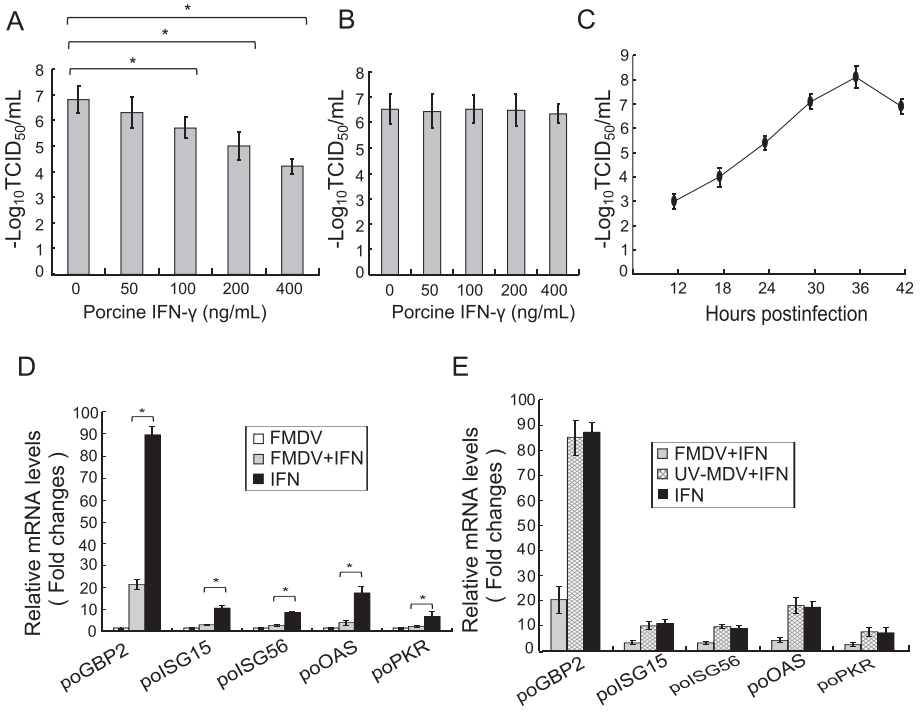

Fig. 1. The anti-FMDV activity of IFN-γ and inhibition of the expression of IFN-γ stimulated genes by FMDV. **A** PK-15 cells were separately pretreated with 0, 50, 100, 200, 400 ng/mL porcine IFN-γ for 5 h and then infected with FMDV O/BY/CHA/2010 at an MOI of 0.1. 24 h later, $TCID_{50}$ was determined on BHK-21 cells. **B** PK-15 cells infected with FMDV O/BY/CHA/2010 at an MOI of 0.1 for 24 h were treated with 0, 50, 100, 200, 400 ng/mL porcine IFN-γ. 5 h later, $TCID_{50}$ was determined on BHK-21 cells. **C** PK-15 cells were infected with FMDV O/BY/CHA/2010 at an MOI of 0.1 and growth kinetics was determined. PK-15 cells were inoculated with FMDV **(D)** or UV-inactivated FMDV **(E)** at an MOI of 0.1 for 24 h and then treated with porcine IFN-γ (200 ng/mL) for 5 h. The mRNA levels of *poGBP2*, *poISG15*, *poISG56*, *poOAS* and *poPKR* were examined using real-time RT-PCR. The levels of relative transcript were shown as relative fold changes, compared with the mock-treated control level of uninfected cells. Data represent the mean ± the standard deviations (error bars) of three independent experiments. *, $P < 0.05$.

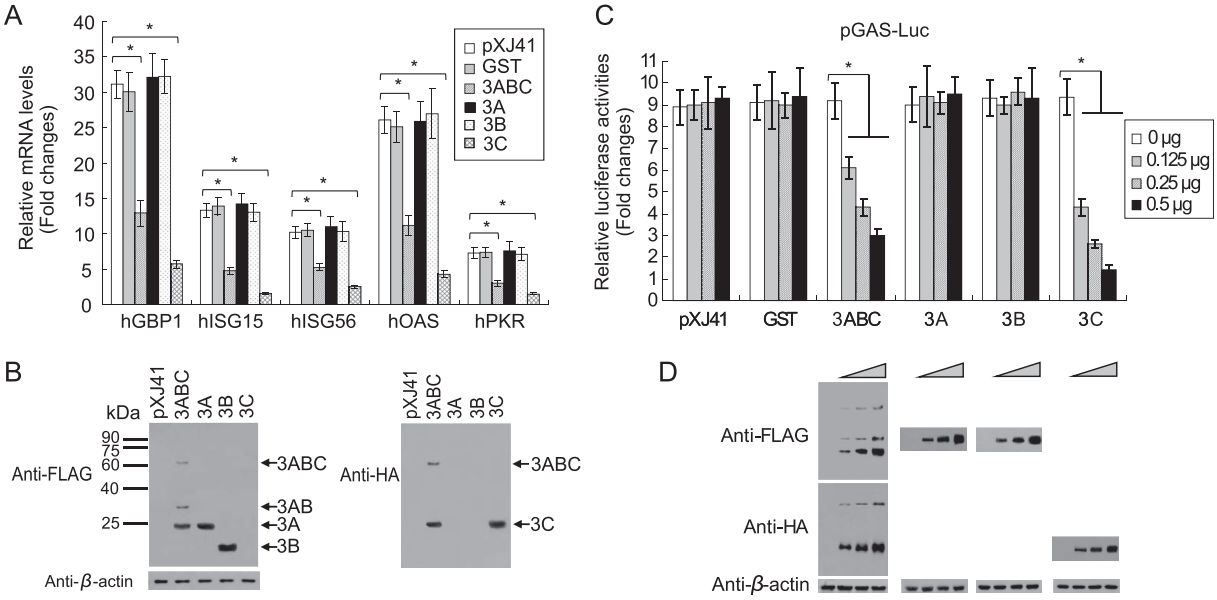

Fig. 2. FMDV 3C^{pro} suppressed ISGs mRNA synthesis and GAS promoter activity of type II IFN signaling. **A** HeLa cells transfected with pXJ41, pXJ41-GST, pXJ41-3ABC, pXJ41-3A, pXJ41-3B or pXJ41-3C were treated with 100 ng/mL of human IFN-γ at 24 h after transfection. 5 h later, the ISGs transcript levels were measured by real-time RT-PCR, with pXJ41 and pXJ41-GST as negative controls. The levels of relative transcript were shown as relative fold changes, compared with the mock-treated control level of uninfected cells. Data represent the mean ± the standard deviations (error bars) of three independent experiments. **B** Expression of 3ABC, 3A, 3B or 3C protein was detected by Western blotting using antibody against FLAG or antibody against HA. β-actin was used as a protein loading control. **C** HeLa cells grown in 12-well plates were cotransfected with 0 μg, 0.125 μg, 0.25 μg or 0.5 μg of pXJ41, pXJ41-GST, pXJ41-3ABC, pXJ41-3A, pXJ41-3B or pXJ41-3C and 0.5 μg of pGAS-Luc as well as 0.05 μg of pRL-TK as an internal control. pXJ41 and pXJ41-GST were worked as negative controls. At 24 h after transfection, cells were treated with 100 ng/mL of human IFN-γ. 16 h later, cells were lysed and reporter expressions were measured using the Dual-Luciferase reporter assay kit (Promega). The values were normalized regarding *Renilla* luciferase activities. Then relative expression levels were calculated and shown as relative fold changes, compared with the mock-treated control of untransfected cells. Data represent the mean ± the standard deviations (error bars) of three independent experiments. **D** Expression of 3ABC, 3A, 3B or 3C protein was detected by Western blotting using antibody against FLAG or antibody against HA. β-actin was used as a protein loading control. *, $P < 0.05$.

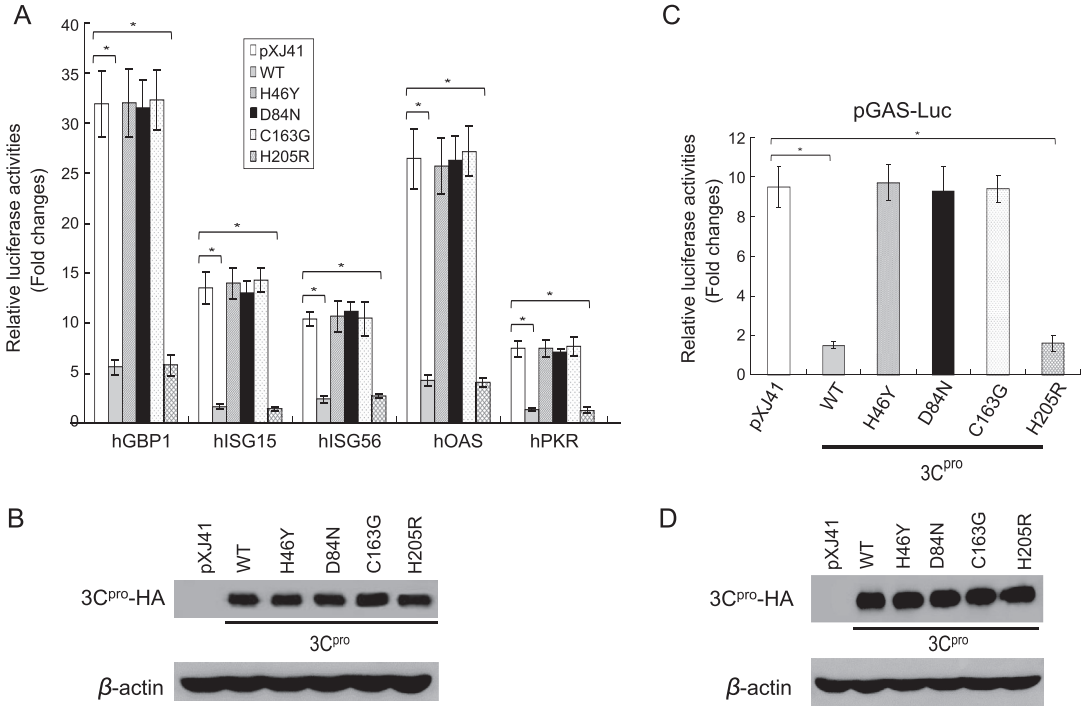

Fig. 3. The catalytic triad H46, D84 and C163 of 3C^{pro} played essential roles in suppressing ISGs mRNA synthesis and GAS promoter activity of type II IFN signaling. **A** HeLa cells transfected with pXJ41, pXJ41-3C or individual mutants of pXJ41-3C were treated with 100 ng/mL human IFN-γ at 24 h after transfection. 5 h later, the hGBP1, hISG15, hISG56, hOAS and hPKR transcript levels were analyzed by real-time RT-PCR as described above. Data represent the means ± the standard deviations (error bars) of three independent experiments, with each experiment in triplicate. **B** Expression of 3C or individual mutant protein was detected by Western blotting using antibody against HA. β-actin was used as a protein loading control. **C** HeLa cells transfected with 0.5 μg of pXJ41, pXJ41-3C or its individual mutants of pXJ41-3C and 0.5 μg of pGAS-Luc as well as 0.05 μg of pRL-TK. At 24 h after transfection, cells were treated with 100 ng/mL human IFN-γ. 16 h later, cells were lysed and reporter expressions were measured using the Dual-Luciferase reporter assay kit as described above. Data represent the mean ± the standard deviations (error bars) of three independent experiments. **D** Expression of 3C or individual mutant protein in HeLa cells transfected with indicated plasmid was detected by Western blotting using antibody against HA. β-actin was used as a protein loading control. *, $P < 0.05$.

mL porcine IFN-γ at 24 h post-infection, viral titers were not significantly decreased (Fig. 1B), demonstrating that virus production was not greatly affected by high concentrations of IFN-γ after the establishment of infection. Under this experimental condition, IFN-γ nearly had no antiviral activity. To ensure that FMDV replication is not already complete before IFN-γ treatment, a growth curve analysis of FMDV without IFN-γ treatment was performed. The results showed that FMDV replication was not yet complete at 24 h post-infection and peaked at 36 h post-infection (Fig. 1C).

Type II IFN signaling regularly leads to increased expression of various cellular genes, including ISG15, ISG56, OAS, PKR and GBP2 (Darnell, Jr. et al., 1994; Aaronson and Horvath, 2002; Shuai and Liu, 2003). To investigate whether FMDV replication affected the expression of these genes, PK-15 cells were inoculated with FMDV or UV-inactivated FMDV for 24 h, and then treated with porcine IFN-γ for 5 h. The mRNA levels were detected using real-time RT-PCR. As seen in Fig. 1D and E, the mRNA levels of poGBP2, poISG15, poISG56, poOAS and poPKR were reduced in FMDV inoculated cells but not UV-inactivated FMDV inoculated cells, indicating that active FMDV replication is needed for the reduction of ISGs transcript after type II IFN stimulation.

3.2. FMDV 3C^{pro} interferes with ISGs mRNA synthesis and GAS promoter activity of type II IFN signaling

Our previous research has shown that 3C^{pro} could interfere with ISGs mRNA synthesis of type I IFN signaling (Du et al., 2014), next we examined whether 3C^{pro} could inhibit the type II IFN signaling. HeLa cells were transfected with pXJ41, pXJ41-GST, pXJ41-3ABC, pXJ41-3A, pXJ41-3B or pXJ41-3C and stimulated with human IFN-γ at 24 h post-transfection, with pXJ41 and pXJ41-GST as negative controls (O'donnell et al., 2012; Hu et al., 2016). The ISGs mRNA levels were obtained by real-time RT-PCR 5 h after IFN-γ stimulation. As seen in Fig. 2A, after normalization to GAPDH, mRNA levels of hGBP1, hISG15, hISG56, hOAS and hPKR in IFN-γ-treated cells transfected with pXJ41 increased 31.1-, 13.3-, 10.2-, 26.1-, 7.3-fold respectively, compared to mock-treated cells. Conversely, in HeLa cells transfected with pXJ41-3C or pXJ41-3ABC after IFN-γ stimulation, mRNA levels of hGBP1, hISG15, hISG56, hOAS and hPKR were 5.7-/12.9-, 1.6-/4.8-, 2.5-/5.3-, 4.3-/11.2-, 1.5-/3.0-fold, respectively, which were significantly lower than those in negative control cells. Expression of 3C showed a 2- to 3-fold greater inhibitory effect than 3ABC, while no inhibitory effect was observed in 3A and 3B expressed cells. 3ABC of FMDV is capable of self-cleavage (Belsham, 2005); 3A, 3AB and 3ABC were detected in 3ABC-transfected cells using antibody against FLAG, while 3C and 3ABC were detected with antibody against HA (Fig. 2B). Since 3ABC was largely cleaved in transfected cells, these results indicate that 3C^{pro} is the protein with 3ABC that mediates the inhibition of type II IFN-mediated ISGs mRNA expression.

In order to detect the effects of FMDV 3C^{pro} on the IFN-γ-induced GAS-mediated response, the plasmids shown in Fig. 2C were cotransfected with GAS-luciferase and *Renilla* luciferase reporters into HeLa cells; pXJ41 and GST were used as negative controls. Upon IFN-γ treatment, GAS promoter activities were inhibited in 3C^{pro}- and 3ABC-expressing cells in a dose-dependent manner, while no inhibitory effect was found in 3A- and 3B-expressing cells, similar to those of the negative controls. In 0.5 μg plasmid transfected cells, the GAS promoter activity in FMDV 3C-expressing cells was 2.1-fold lower than that in 3ABC-transfected cells, while the GAS promoter activity in 3ABC-expressing cells was approximately 3.1-fold lower than that in pXJ41-transfected cells. Evidently, 3C showed a stronger inhibitory effect than 3ABC. Successful protein expression in 3ABC, 3A, 3B or 3C-transfected cells was detected by Western blotting using antibody against FLAG or HA (Fig. 2D). These results demonstrate that FMDV 3C^{pro} is responsible for 3ABC-mediated suppression of GAS promoter activity.

3.3. The catalytic triad of H46, D84 and C163 of 3C^{pro} is essential for FMDV 3C^{pro} to suppress ISGs mRNA and GAS promoter activities of type II IFN signaling

According to previous reports, the catalytic triad of H46, D84, and C163 of FMDV 3C^{pro} plays important roles in its protease activity (Grubman et al., 1995; Birtley et al., 2005), and we also found that the protease activity of 3C^{pro} was involved in antagonizing the type I IFN signaling pathway (Du et al., 2014). To determine whether these residues affect the type II IFN signaling pathway, real-time RT-PCR and luciferase assays were conducted. As shown in Fig. 3A and C, the wild-type (WT) 3C and 3C-H205R mutant strongly suppressed the mRNA levels of ISGs and GAS promoter activities of type II IFN signaling. In contrast, no suppression was found in cells transfected with H46Y, D84N, C163G mutants, or the pXJ41 vector control. These data indicate that the catalytic triad of H46, D84, and C163 of 3C^{pro} are essential for FMDV 3C^{pro} antagonism of the type II IFN signaling pathway. Fig. 3B and D showed the successful expression of 3C^{pro} or its mutants in two different experiments.

3.4. FMDV 3C^{pro} does not alter the protein level, phosphorylation or homodimerization of STAT1

To investigate the protein expression of STAT1 in the presence of 3C^{pro}, HeLa cells were transfected with pXJ41-3C and treated with

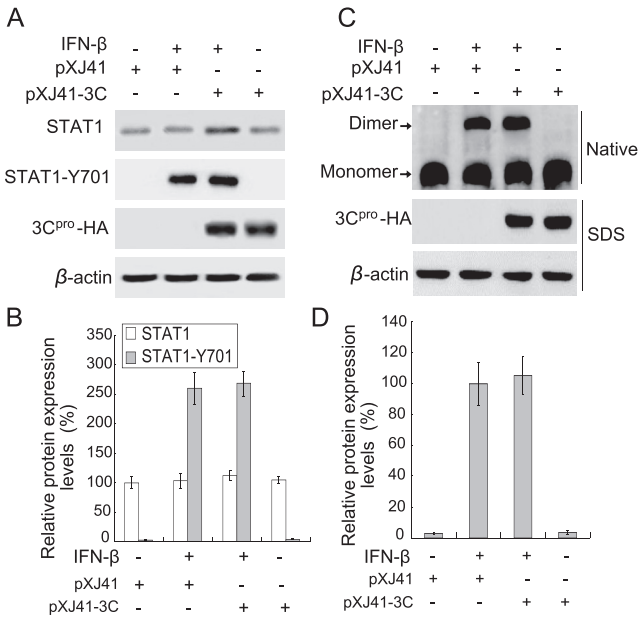

Fig. 4. STAT1 expression level, phosphorylation status and its homodimer formation in FMDV 3C^{pro}-expressing cells after IFN-γ stimulation. **A** HeLa cells transfected with pXJ41 or pXJ41-3C were treated with 100 ng/mL human IFN-γ for 1 h at 24 h after transfection and collected for Western blotting with antibody against STAT1 (top panel), phospho-STAT1 (STAT1-Y701, panel 2) or HA (panel 3), respectively. Antibody against β-actin (bottom panel) was used as a protein loading control. **B** Densitometric analysis of the digital image in (**A**). Intensities of the band were normalized with that of β-actin. **C** Cells transfected with pXJ41 or pXJ41-3C were treated with human 100 ng/mL IFN-γ for 1 h at 24 h post-transfection. Samples were lysed and subjected to native-PAGE and immunoblotting with antibody against STAT1 (top panel). Expression of 3C^{pro} was detected by SDS-PAGE and immunoblotting with antibody against HA (panel 2), with β-actin as a loading control (bottom panel). **D** Densitometric analysis of the digital image in (**C**). Intensities of the band were normalized with that of β-actin. Data represent the mean ± the standard deviations (error bars) of three independent experiments.

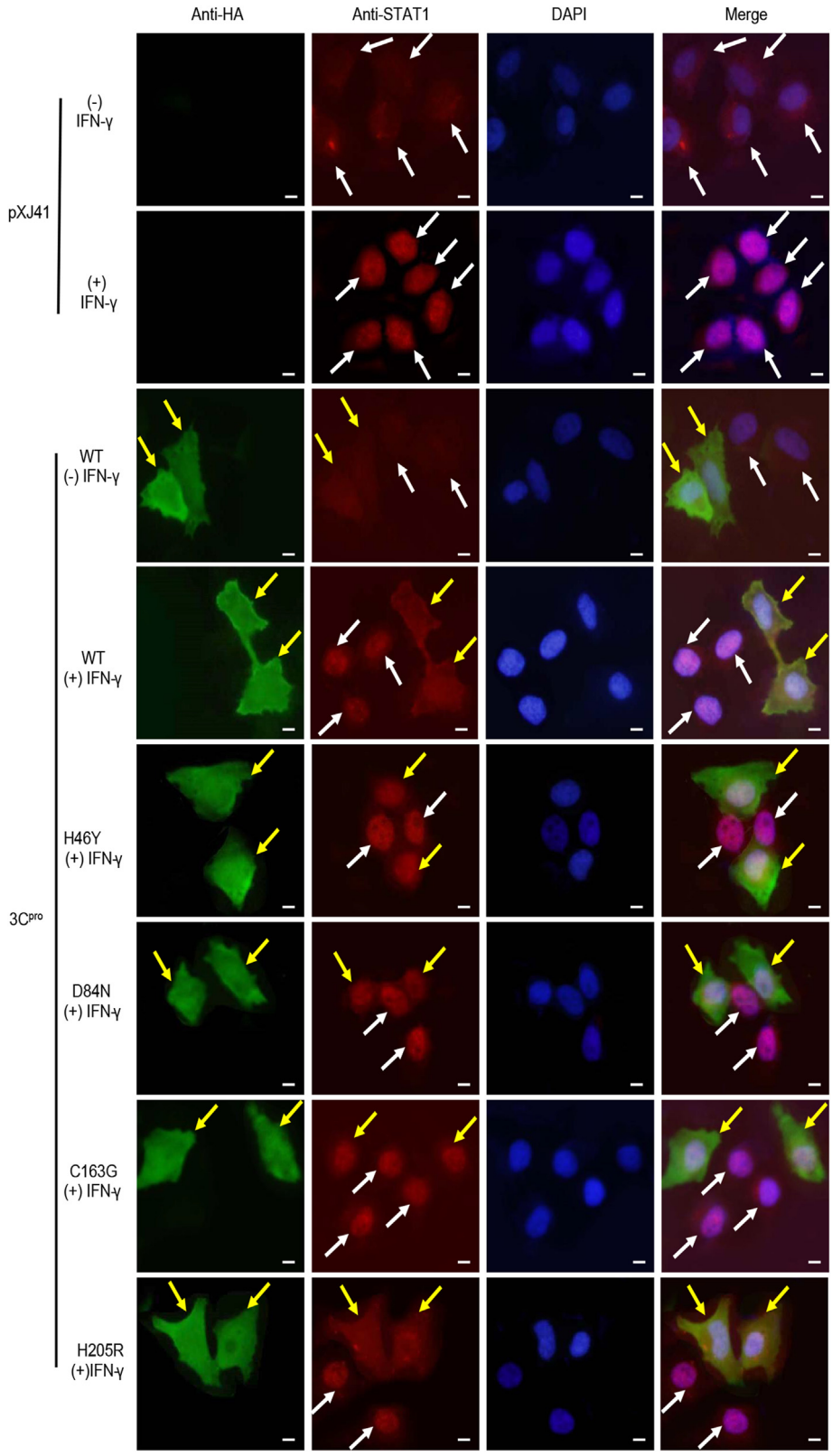

Fig. 5. FMDV $3C^{pro}$ inhibits nuclear translocation of STAT1 as directed by IFA. HeLa cells transfected with pXJ41, pXJ41-3C, or individual mutants of pXJ41-3C were either left untreated (−) or treated (+) with human 100 ng/mL IFN-γ for 1 h at 18 h post-transfection. Cells were fixed, and an IFA was conducted. Yellow arrows indicate WT or mutated $3C^{pro}$-expressing cells, and white arrows indicate untransfected cells. Scale bar, 10 μm.

human IFN-γ. Western blotting analysis revealed that STAT1 expression was unchanged in 3C^{pro}-transfected cells compared to pXJ41-transfected cells (Fig. 4A, STAT1, and B), indicating that FMDV 3C^{pro} did not alter the protein level of STAT1.

After IFN-γ binds to its receptor (IFNGR) and activates JAKs, STAT1 forms a homodimer and translocates to the nucleus where it is phosphorylated and plays a key role in mediating IFN-γ-induced antiviral responses (Didcock et al., 1999). To explore whether the phosphorylation of STAT1 was interfered by FMDV 3C^{pro}, lysates from 3C^{pro}-transfected cells were explored using Western blotting with phospho-STAT1 (STAT1-Y701) antibody. The level of phosphorylated STAT1 was greatly increased after IFN-γ treatment, and the extent of phosphorylation was not affected by the presence of 3C^{pro} (Fig. 4A, STAT1-Y701, and B). In mock-treated cells, the level of phosphorylated STAT1 was below the detectable level. These results demonstrate that FMDV 3C^{pro} does not alter the phosphorylation status of STAT1 after IFN-γ stimulation.

Next, in order to detect the homodimerization status of STAT1 in 3C^{pro}-transfected cells, we performed native-PAGE and immunoblotting with antibody against STAT1. STAT1 homodimer was detected both in IFN-γ-treated pXJ41-transfected and pXJ41-3C-transfected cells with no obvious difference between them (Fig. 4C and D). These data demonstrate that the homodimerization of STAT1 in 3C^{pro}-transfected cells is not significantly affected.

3.5. FMDV 3C^{pro} inhibits the nuclear translocation of STAT1

Once activated, STAT1 homogenizes and translocates to nucleus and binds GAS to initiate gene transcription (Platanias, 2005). Compared to the negative control, ISGs mRNA and GAS promoter activity in 3C^{pro}-transfected cells treated with IFN-γ were decreased significantly, but the protein level, phosphorylation, and homodimerization of STAT1 were not affected, leading us to examine the effect of 3C^{pro} on STAT1 nuclear translocation. HeLa cells transfected with pXJ41, pXJ41-3C, or individual mutants were treated with human IFN-γ at 18 h post-transfection and an IFA was performed. In pXJ41-transfected cells or cells expressing WT 3C^{pro} without stimulation, STAT1 was distributed in the cytoplasm and nucleus (Fig. 5, first and third rows). After IFN-γ stimulated, STAT1 was predominantly found in the nucleus in pXJ41-transfected cells (Fig. 5, second row). However, the majority of the STAT1 remained in the cytoplasm of cells expressing WT 3C^{pro} and the 3C^{pro}-H205R mutant after IFN-γ stimulation (Fig. 5, fourth and eighth rows). Interestingly, the 3C^{pro} mutants of H46Y, D84N, and C163G could not inhibit STAT1 nuclear translocation (Fig. 5, fifth, sixth

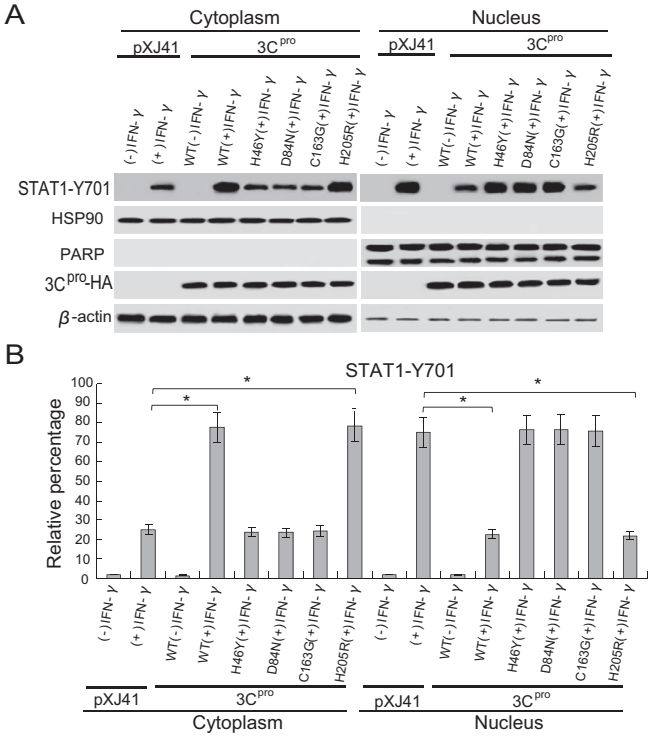

Fig. 6. Phosphorylated STAT1 in nucleus and cytoplasm. **A** Western blot analysis of phosphorylated STAT1 in nucleus and cytoplasm fraction. HeLa cells were performed for nuclear and cytoplasmic separation after human IFN-γ treatment for 1 h. Samples were analyzed by Western blotting using antibody against STAT1-Y701 (top panel), antibodies against HSP90 and PARP were used as cytoplasmic and nuclear protein marker respectively. 3C^{pro} expression of FMDV was detected using antibody against HA (panel 4), with antibody against β-actin as a loading control (bottom panel). **B** Densitometric analysis of the band of phosphorylated STAT1 in nucleus and cytoplasm. Intensities of the band were shown as the relative percentage of the total density of their counterpart, cytoplasmic and nuclear fractions normalized with HSP90 and PARP respectively. Data represent the mean ± the standard deviations (error bars) of three experiments. -: without IFN-γ treatment, +: with IFN-γ treatment. *, $P < 0.05$.

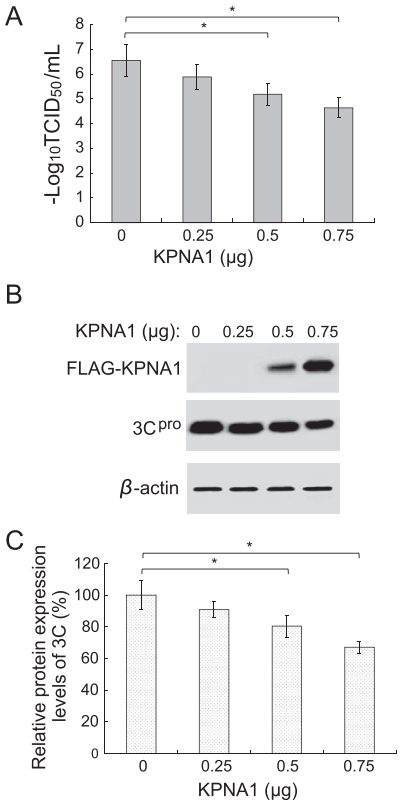

Fig. 7. The antiviral activity of IFN-γ against FMDV was recovered by KPNA1 overexpression. **A** PK-15 cells infected with FMDV O/BY/CHA/2010 at an MOI of 0.1 for 2 h were transfected with 0 μg, 0.25 μg, 0.5 μg or 0.75 μg of pXJ41-FLAG-KPNA1. Empty vector pXJ41 was used to ensure that the total amount of transfected plasmid DNA in each group was 0.75 μg. At 24 h after infection, cells were treated with 400 ng/mL porcine IFN-γ. 5 h later, $TCID_{50}$ was determined on BHK-21 cells. Data represent the mean ± the standard deviations (error bars) of three experiments. **B** Expression of KPNA1 (top panel) or FMDV 3C^{pro} (middle panel) in PK-15 cells detected by Western blotting using antibody against FLAG or rabbit 3C serum, with β-actin as a loading control (bottom panel). **C** Densitometric analysis of the digital image of FMDV 3C^{pro}. The band intensities normalized with β-actin were suggested as relative protein expression. Data represent the mean ± the standard deviations (error bars) of three experiments. *, $P < 0.05$.

and seventh rows). This observation was further confirmed by nuclear and cytoplasmic fractionation of the cells as described previously (Du et al., 2014). As shown in Fig. 6A and B, phosphorylated STAT1, STAT1-Y701, was detected both in nuclear and cytoplasmic fractions in cells stimulated with IFN-γ. In H46Y, D84N and C163G mutated $3C^{pro}$-transfected cells, more STAT1-Y701 was detected in the nuclear fraction than in the cytoplasmic fraction, similar to pXJ41-transfected cells. However, in WT $3C^{pro}$ and H205R mutated $3C^{pro}$-transfected cells, more STAT1-Y701 was present in the cytoplasmic fraction rather than in the nuclear fraction. The cytoplasmic protein marker HSP90 and nuclear protein marker PARP were detected in the appropriate fraction, showing that cellular fractionation was successful (Fig. 6A, HSP90 and PARP). FMDV $3C^{pro}$ was detected in both the cytoplasm and nucleus (Fig. 6A, $3C^{pro}$-HA), similar to our previous reports (Du et al., 2014). As an actin protein, β-actin is detected mainly in cytoplasm (Fig. 6A).

3.6. FMDV 3C degrades KPNA1 of type II IFN-stimulated JAK-STAT signaling pathway

Our previous study showed that the protease activity of $3C^{pro}$ induced the degradation of KPNA1 and thus blocked STAT1/STAT2 nuclear translocation and antagonized the type I IFN signaling pathway (Du et al., 2014). To further explore the mechanism of $3C^{pro}$ in degrading KPNA1 and antagonizing the type II IFN-stimulated JAK-STAT signaling pathway, PK-15 cells were infected with 0.1 MOI of FMDV O/BY/CHA/2010 for 2 h and then transfected with the indicated dose of pXJ41-FLAG-KPNA1 plasmid. 22 h later, porcine IFN-γ (400 ng/mL) was added and virus titers were measured. As shown in Fig. 7A, with increasing amounts of KPNA1 transfection, viral titers were decreased, overcoming the effects of FMDV 3C inhibitory activity on IFN-γ. The expression of KPNA1 and FMDV $3C^{pro}$ was detected using anti-FLAG antibody and rabbit anti-3C serum by Western blotting. Interestingly, no

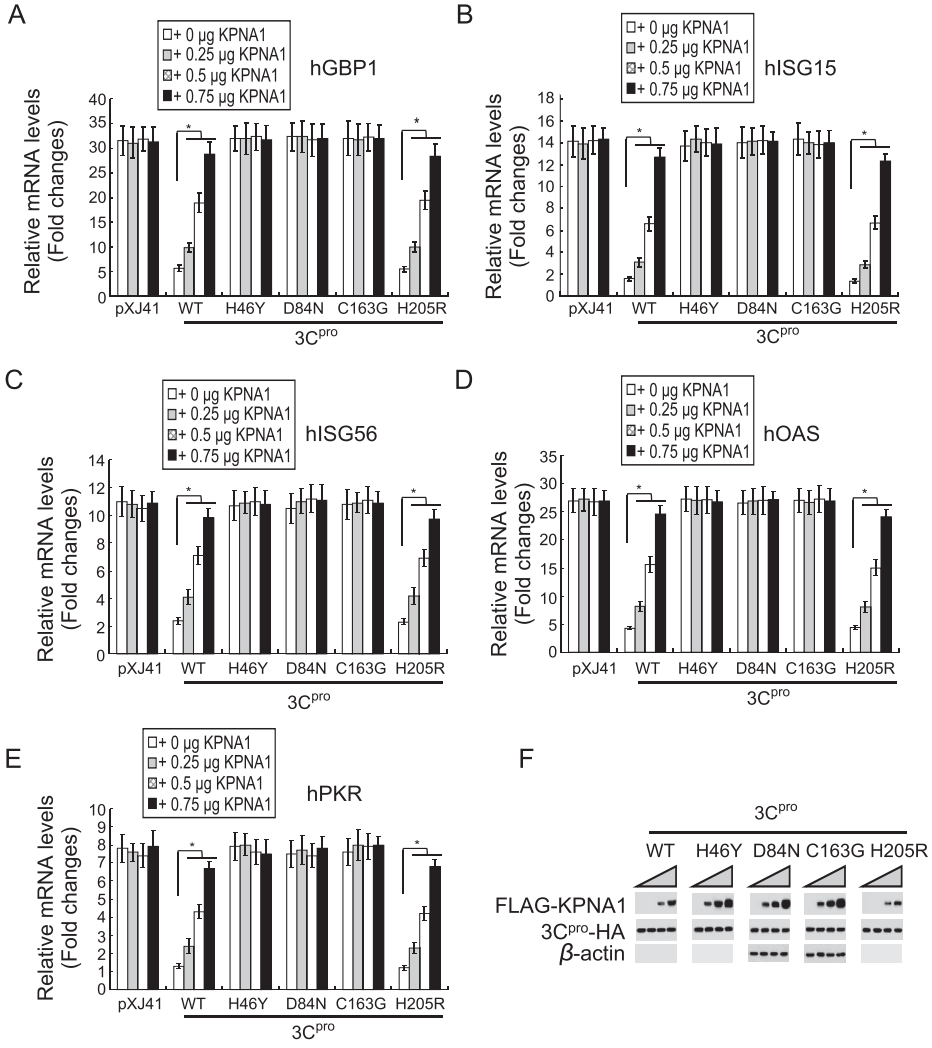

Fig. 8. ISGs mRNA level of type II IFN signaling is associated with FMDV 3C protease activity in degrading KPNA1. HeLa cells cotransfected with increased dose of pXJ41-FLAG-KPNA1 and pXJ41-3C or its mutants were treated with 100 -ng/mL human IFN-γ at 24 h post-transfection. 5 h later, the mRNA levels of hGBP1 (**A**), hISG15 (**B**), hISG56 (**C**), hOAS (**D**) and hPKR (**E**) were detected by real-time RT-PCR as described above. Data represent the mean ± the standard deviations (error bars) of three independent experiments. **F** Expression of KPNA1, 3C or its mutant protein was measured by Western blotting using antibody against FLAG or HA. β-actin was used as a protein loading control. *, $P < 0.05$.

FLAG-KPNA1 was detected in 0.25 μg-KPNA1 transfected cells (Fig. 7B), suggesting that 3C degraded the exogenously transfected KPNA1. With the increase of exogenous KPNA1, there was not enough 3C to degrade exogenous KPNA1, leading to a dose-dependent decrease of FMDV titer and FMDV 3C protein level (Fig. 7A and B $3C^{pro}$ and C). These results suggested the important role of FMDV 3C inducing KPNA1 degradation in antagonizing the type II IFN-stimulated JAK-STAT signaling pathway.

3.7. ISGs mRNA and GAS promoter activities of type II IFN signaling are associated with FMDV 3C protease activity in degrading KPNA1

Next, we examined the effects of increased KPNA1 expression on ISGs mRNA levels and GAS promoter activity after the type II IFN signaling in the presence of $3C^{pro}$. HeLa cells were cotransfected with increased amount of pXJ41-FLAG-KPNA1 along with pXJ41-3C or its mutants, and then treated with human IFN-γ at 24 h post-transfection. The mRNA levels of ISGs and GAS promoter activity were analyzed. The mRNA levels of hGBP1, hISG15, hISG56, hOAS and hPKR in WT-$3C^{pro}$ and $3C^{pro}$-H205R mutant transfected cells recovered with increased KPNA1 expression. As expected, there were no effects in cells expressing H46Y, D84N and C163G mutants of $3C^{pro}$ (Fig. 8). GAS promoter activities were also enhanced in WT-$3C^{pro}$ and $3C^{pro}$-H205R mutant transfected cells with increased KPNA1 expression (Fig. 9). These results further confirmed the essential role of FMDV 3C protease activity in degrading KPNA1 and antagonizing the type II IFN-stimulated JAK-STAT signaling pathway.

4. Discussion

IFNs are a group of secreted cytokines that elicit extremely powerful antiviral, antiproliferative and immunomodulatory effects (Randall and Goodbourn, 2008). To escape the IFN immune system, viruses develop strategies to antagonize the host innate immunity. FMDV, causing economically important disease, has adopted tactics to circumvent the host IFN signaling (De Los Santos et al., 2006; De Los Santos et al., 2007; Wang et al., 2010; Wang et al., 2012; Du et al., 2014). Herein, we first show that FMDV $3C^{pro}$ interferes with the type II IFN signaling pathway by degrading KPNA1 and thus blocking STAT1 nuclear translocation (Figs. 5–7). Further, we provide evidence that 3C protease activity plays an essential role in degrading KPNA1 and thus inhibits ISGs mRNA and GAS promoter activities (Figs. 8 and 9). Up to now, we find FMDV $3C^{pro}$ not only antagonizes type I IFN signaling pathway (Du et al., 2014), but also inhibits type II IFN signaling pathway. As IFN-γ is the only member of type II IFN and is critical for innate and adaptive immunity against viral infections (Schoenborn and Wilson, 2007), our results suggest the essential role of $3C^{pro}$ in FMDV counteracting host innate immune response and facilitating FMDV replication in host cells.

Multiple studies have proved that FMDV can antagonize type I IFN signaling pathway (De Los Santos et al., 2006; De Los Santos et al., 2007; Wang et al., 2010; Wang et al., 2012; Du et al., 2014). It was also reported that FMDV structural protein VP3 degrades Janus kinase 1 and inhibits type II IFN-stimulated JAK-STAT pathway (Li et al., 2016). In order to further investigate whether FMDV could interfere with type II IFN signaling pathway, we explored the antiviral activity of IFN-γ during FMDV infection. Results showed that IFN-γ has anti-FMDV activity prior to FMDV infection (Fig. 1A) but has no antiviral activity when PK-15 cells were treated with IFN-γ after infection (Fig. 1B).

Previously, we and others demonstrated that FMDV $3C^{pro}$ inhibits type I IFN signaling pathway (Wang et al., 2012; Du et al., 2014). To determine whether FMDV $3C^{pro}$ antagonizes the type II IFN signaling pathway or not, we explored type II IFN-stimulated JAK-STAT pathway in $3C^{pro}$ expressed cells. Results show that $3C^{pro}$ contributes to 3ABC--mediated suppression of the ISGs transcript levels and GAS promoter activity (Fig. 2). The catalytic triad H46, D84 and C163 of $3C^{pro}$ are integral for FMDV $3C^{pro}$ to inhibit ISGs mRNA and GAS promoter activities (Fig. 3).

IFN-γ induces tyrosine phosphorylation of STAT1, generating SH2 domain-mediated homodimers (gamma-activated factor, or GAF) that translocate to the nucleus and bind to GAS (Young et al., 2000; Begitt et al., 2014). Many viruses may interfere with the IFN-γ-activated

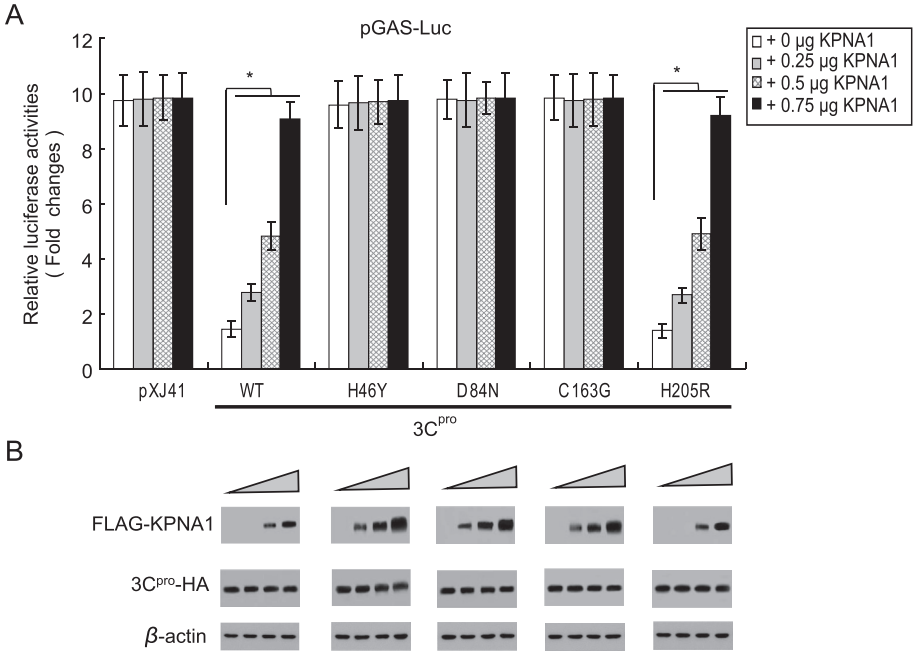

Fig. 9. GAS promoter activity of type II IFN signaling is associated with FMDV 3C protease activity in degrading KPNA1. **A** HeLa cells cotransfected with increased dose of pXJ41-FLAG-KPNA1 and pXJ41-3C or its mutants and pGAS-Luc as well as pRL-TK for 24 h were incubated with 100 ng/mL human IFN-γ for 16 h. Luciferase assay was performed as described above. Data represent the mean ± the standard deviations (error bars) of three experiments. **B** Expression of KPNA1, 3C or its mutant protein was measured by Western blotting using antibody against FLAG or HA. β-actin was used as a protein loading control. *, $P < 0.05$.

JAK-STAT signaling pathway via inducing the degradation of STAT1 (Yokosawa et al., 1998; Didcock et al., 1999; Young et al., 2000; Andrejeva et al., 2002; Kubota et al., 2005), sequestration of STAT1, blocking its phosphorylation (Rodriguez et al., 2002; Devaux et al., 2007; Simmons et al., 2009), inhibiting STAT1 nuclear translocation (Mcbride et al., 2002; Rodriguez et al., 2002; Palosaari et al., 2003; Rodriguez et al., 2003; Reid et al., 2006; Montgomery and Johnston, 2007; Simmons et al., 2009), or inhibiting a process after nuclear translocation of GAF (Miller et al., 1998; Didcock et al., 1999; Vidy et al., 2007). We showed that FMDV $3C^{pro}$ does not affect the amounts of STAT1 in IFN-γ-treated cells, nor alter the IFN-induced phosphorylation of STAT1 (Fig. 4A and B). Furthermore, $3C^{pro}$ does not change the homodimerization of STAT1 (Fig. 4C and D). Interestingly, $3C^{pro}$ blocks STAT1 translocated to nuclear, during which, the protease activity of $3C^{pro}$ is essential (Figs. 5 and 6).

There are a variety of regulations during GAF translocated to the nucleus. After being phosphorylated, STAT1 exposes a nuclear localization signal (NLS) to recruit importin-α receptors. Importin-α5, also called KPNA1, is known to bind and shuttle STAT1 to the nuclear pore complex to regulate its nuclear import (Mcbride et al., 2002). Our previous study showed that $3C^{pro}$ of FMDV induces the degradation of KPNA1 and thus inhibits type I IFN-stimulated JAK-STAT signaling pathway (Du et al., 2014). We examined the function of KPNA1 during FMDV infection in IFN-γ-treated PK-15 cells. As we expected, cells transfected with KPNA1 recovered the antiviral activity of IFN-γ against FMDV (Fig. 7), ISGs mRNA synthesis and GAS promoter activity (Figs. 8 and 9). With the increase of KPNA1, there is insufficient 3C to degrade KPNA1, which leads to the recovery of IFN-γ antiviral activity and decreased FMDV titers, suggesting the importance of 3C degradation of KPNA1 in antagonizing the type II IFN signaling pathway (Fig. 7). These data were not shown in our previous report of FMDV $3C^{pro}$ degrading KPNA1 and inhibiting type I IFN signaling pathway (Du et al., 2014), and above all, the stimulant for each IFN signaling pathway is different.

5. Conclusions

In summary, we have first elucidated the mechanism of FMDV non-structural protein 3C mediated-inhibition of IFN-γ-stimulated JAK-STAT signaling pathway. The KPNA1 degradation by FMDV $3C^{pro}$ presents the first example of a viral immune evasion mechanism during type II IFN signaling pathway. Our research reveals a novel mechanism developed by FMDV non-structural protein to antagonize host type II IFN signaling.

Data availability

The authors confirm that the data supporting the findings of this study are available within the article.

Ethics statement

This article does not contain any studies with human or animal subjects performed by any of the authors.

Author contributions

Xiangju Wu: conceptualization, data curation, investigation, writing-original draft, writing-review & editing. Lei Chen: data curation, formal analysis, methodology, resources, writing-original draft. Chao Sui: data curation, investigation, methodology. Yue Hu: investigation, supervision. Dandan Jiang: data curation, validation. Fan Yang: data curation, methodology, resources. Laura C. Miller: formal analysis, visualization. Juntong Li: data curation, software. Xiaoyan Cong: validation, resources. Nataliia Hrabchenko: formal analysis, methodology. Changhee Lee: formal analysis, resources. Yijun Du: conceptualization, data curation, formal analysis, funding acquisition, methodology, project administration, supervision, writing-review & editing. Jing Qi: data curation, methodology, project administration, resources, software, supervision, writing-review & editing.

Conflict of interest

The authors declare that they have no conflict of interest.

Acknowledgements

The authors would like to thank Dr. Stanley Perlman, University of Iowa, for his valuable help on discussing data and correcting the manuscript. This work was supported by the National Key Research and Development Program of China (2021YFD1800300), Natural Science Foundation of Shandong Province (ZR2021ZD08, ZR2020KC005, ZR2021MC139, ZR2020QC196), National Natural Science Foundation of China (32102710), and the Agricultural Scientific and Technological Innovation Project of Shandong Academy of Agricultural Sciences (CXGC2023A21, CXGC2021B03, CXGC2022A17).

Appendix A. Supplementary data

Supplementary data to this article can be found online at https://doi.org/10.1016/j.virs.2023.03.003.

References

Aaronson, D.S., Horvath, C.M., 2002. A road map for those who don't know JAK-STAT. Science 296, 1653–1655.
Andrejeva, J., Poole, E., Young, D.F., Goodbourn, S., Randall, R.E., 2002. The p127 subunit (DDB1) of the UV-DNA damage repair binding protein is essential for the targeted degradation of STAT1 by the V protein of the paramyxovirus simian virus 5. J. Virol. 76, 11379–11386.
Begitt, A., Droescher, M., Meyer, T., Schmid, C.D., Baker, M., Antunes, F., Knobeloch, K.P., Owen, M.R., Naumann, R., Decker, T., Vinkemeier, U., 2014. STAT1-cooperative DNA binding distinguishes type 1 from type 2 interferon signaling. Nat. Immunol. 15, 168–176.
Belsham, G.J., 2005. Translation and replication of FMDV RNA. Curr. Top. Microbiol. Immunol. 288, 43–70.
Birtley, J.R., Knox, S.R., Jaulent, A.M., Brick, P., Leatherbarrow, R.J., Curry, S., 2005. Crystal structure of foot-and-mouth disease virus 3C protease. New insights into catalytic mechanism and cleavage specificity. J. Biol. Chem. 280, 11520–11527.
Darnell Jr., J.E., Kerr, I.M., Stark, G.R., 1994. Jak-STAT pathways and transcriptional activation in response to IFNs and other extracellular signaling proteins. Science 264, 1415–1421.
De Los Santos, T., De Avila Botton, S., Weiblen, R., Grubman, M.J., 2006. The leader proteinase of foot-and-mouth disease virus inhibits the induction of beta interferon mRNA and blocks the host innate immune response. J. Virol. 80, 1906–1914.
De Los Santos, T., Diaz-San Segundo, F., Grubman, M.J., 2007. Degradation of nuclear factor kappa B during foot-and-mouth disease virus infection. J. Virol. 81, 12803–12815.
Devaux, P., Von Messling, V., Songsungthong, W., Springfeld, C., Cattaneo, R., 2007. Tyrosine 110 in the measles virus phosphoprotein is required to block STAT1 phosphorylation. Virology 360, 72–83.
Didcock, L., Young, D.F., Goodbourn, S., Randall, R.E., 1999. The V protein of simian virus 5 inhibits interferon signalling by targeting STAT1 for proteasome-mediated degradation. J. Virol. 73, 9928–9933.
Du, Y., Bi, J., Liu, J., Liu, X., Wu, X., Jiang, P., Yoo, D., Zhang, Y., Wu, J., Wan, R., Zhao, X., Guo, L., Sun, W., Cong, X., Chen, L., Wang, J., 2014. $3C^{pro}$ of foot-and-mouth disease virus antagonizes the interferon signaling pathway by blocking STAT1/STAT2 nuclear translocation. J. Virol. 88, 4908–4920.
Dunn, G.P., Ikeda, H., Bruce, A.T., Koebel, C., Uppaluri, R., Bui, J., Chan, R., Diamond, M., White, J.M., Sheehan, K.C., Schreiber, R.D., 2005. Interferon-gamma and cancer immunoediting. Immunol. Res. 32, 231–245.
Dunn, G.P., Koebel, C.M., Schreiber, R.D., 2006. Interferons, immunity and cancer immunoediting. Nat. Rev. Immunol. 6, 836–848.
Fros, J.J., Liu, W.J., Prow, N.A., Geertsema, C., Ligtenberg, M., Vanlandingham, D.L., Schnettler, E., Vlak, J.M., Suhrbier, A., Khromykh, A.A., Pijlman, G.P., 2010. Chikungunya virus nonstructural protein 2 inhibits type I/II interferon-stimulated JAK-STAT signaling. J. Virol. 84, 10877–10887.
Grubman, M.J., 1980. The 5' end of foot-and-mouth disease virion RNA contains a protein covalently linked to the nucleotide pUp. Arch. Virol. 63, 311–315.
Grubman, M.J., Baxt, B., 2004. Foot-and-mouth disease. Clin. Microbiol. Rev. 17, 465–493.
Grubman, M.J., Zellner, M., Bablanian, G., Mason, P.W., Piccone, M.E., 1995. Identification of the active-site residues of the 3C proteinase of foot-and-mouth disease virus. Virology 213, 581–589.

Hu, Y., Cong, X., Chen, L., Qi, J., Wu, X., Zhou, M., Yoo, D., Li, F., Sun, W., Wu, J., Zhao, X., Chen, Z., Yu, J., Du, Y., Wang, J., 2016. Synergy of TLR3 and 7 ligands significantly enhances function of DCs to present inactivated PRRSV antigen through TRIF/MyD88-NF-κB signaling pathway. Sci. Rep. 6, 23977.
Ikeda, H., Old, L.J., Schreiber, R.D., 2002. The roles of IFN gamma in protection against tumor development and cancer immunoediting. Cytokine Growth Factor Rev. 13, 95–109.
Jamal, S.M., Belsham, G.J., 2018. Molecular epidemiology, evolution and phylogeny of foot-and-mouth disease virus. Infect. Genet. Evol. 59, 84–98.
Kotenko, S.V., 2011. IFN-lambdas. Curr. Opin. Immunol. 23, 583–590.
Kubota, T., Yokosawa, N., Yokota, S., Fujii, N., Tashiro, M., Kato, A., 2005. Mumps virus V protein antagonizes interferon without the complete degradation of STAT1. J. Virol. 79, 4451–4459.
Kulkarni, A., Ganesan, P., O'donnell, L.A., 2016. Interferon gamma: influence on neural stem cell function in neurodegenerative and neuroinflammatory disease. Clin. Med. Insights Pathol. 9, 9–19.
Lang, C., Hildebrandt, A., Brand, F., Opitz, L., Dihazi, H., Luder, C.G., 2012. Impaired chromatin remodelling at STAT1-regulated promoters leads to global unresponsiveness of Toxoplasma gondii-infected macrophages to IFN-gamma. PLoS Pathog. 8, e1002483.
Lasfar, A., Cook, J.R., Cohen Solal, K.A., Reuhl, K., Kotenko, S.V., Langer, J.A., Laskin, D.L., 2014. Critical role of the endogenous interferon ligand-receptors in type I and type II interferons response. Immunology 142, 442–452.
Li, D., Wei, J., Yang, F., Liu, H.N., Zhu, Z.X., Cao, W.J., Li, S., Liu, X.T., Zheng, H.X., Shu, H.B., 2016. Foot-and-mouth disease virus structural protein VP3 degrades Janus kinase 1 to inhibit IFN-γ signal transduction pathways. Cell Cycle 15, 850–860.
Mcbride, K.M., Banninger, G., Mcdonald, C., Reich, N.C., 2002. Regulated nuclear import of the STAT1 transcription factor by direct binding of importin-alpha. EMBO J. 21, 1754–1763.
Miller, D.M., Rahill, B.M., Boss, J.M., Lairmore, M.D., Durbin, J.E., Waldman, J.W., Sedmak, D.D., 1998. Human cytomegalovirus inhibits major histocompatibility complex class II expression by disruption of the Jak/Stat pathway. J. Exp. Med. 187, 675–683.
Montgomery, S.A., Johnston, R.E., 2007. Nuclear import and export of Venezuelan equine encephalitis virus nonstructural protein 2. J. Virol. 81, 10268–10279.
Mori, M., Yoneyama, M., Ito, T., Takahashi, K., Inagaki, F., Fujita, T., 2004. Identification of Ser-386 of interferon regulatory factor 3 as critical target for inducible phosphorylation that determines activation. J. Biol. Chem. 279, 9698–9702.
O'donnell, L.A., Conway, S., Rose, R.W., Nicolas, E., Slifker, M., Balachandran, S., Rall, G.F., 2012. STAT1-independent control of a neurotropic measles virus challenge in primary neurons and infected mice. J. Immunol. 188, 1915–1923.
Palosaari, H., Parisien, J.P., Rodriguez, J.J., Ulane, C.M., Horvath, C.M., 2003. STAT protein interference and suppression of cytokine signal transduction by measles virus V protein. J. Virol. 77, 7635–7644.
Pizzi, M., 1950. Sampling variation of the fifty percent end-point, determined by the Reed-Muench (Behrens) method. Hum. Biol. 22, 151–190.
Platanias, L.C., 2005. Mechanisms of type-I- and type-II-interferon-mediated signalling. Nat. Rev. Immunol. 5, 375–386.
Randall, R.E., Goodbourn, S., 2008. Interferons and viruses: an interplay between induction, signalling, antiviral responses and virus countermeasures. J. Gen. Virol. 89, 1–47.
Reid, S.P., Leung, L.W., Hartman, A.L., Martinez, O., Shaw, M.L., Carbonnelle, C., Volchkov, V.E., Nichol, S.T., Basler, C.F., 2006. Ebola virus VP24 binds karyopherin alpha1 and blocks STAT1 nuclear accumulation. J. Virol. 80, 5156–5167.
Robertson, B.H., Grubman, M.J., Weddell, G.N., Moore, D.M., Welsh, J.D., Fischer, T., Dowbenko, D.J., Yansura, D.G., Small, B., Kleid, D.G., 1985. Nucleotide and amino acid sequence coding for polypeptides of foot-and-mouth disease virus type A12. J. Virol. 54, 651–660.
Rodriguez, J.J., Parisien, J.P., Horvath, C.M., 2002. Nipah virus V protein evades alpha and gamma interferons by preventing STAT1 and STAT2 activation and nuclear accumulation. J. Virol. 76, 11476–11483.
Rodriguez, J.J., Wang, L.F., Horvath, C.M., 2003. Hendra virus V protein inhibits interferon signaling by preventing STAT1 and STAT2 nuclear accumulation. J. Virol. 77, 11842–11845.
Schoenborn, J.R., Wilson, C.B., 2007. Regulation of interferon-gamma during innate and adaptive immune responses. Adv. Immunol. 96, 41–101.
Shuai, K., Liu, B., 2003. Regulation of JAK-STAT signalling in the immune system. Nat. Rev. Immunol. 3, 900–911.
Simmons, J.D., White, L.J., Morrison, T.E., Montgomery, S.A., Whitmore, A.C., Johnston, R.E., Heise, M.T., 2009. Venezuelan equine encephalitis virus disrupts STAT1 signaling by distinct mechanisms independent of host shutoff. J. Virol. 83, 10571–10581.
Stenfeldt, C., Diaz-San Segundo, F., De Los Santos, T., Rodriguez, L.L., Arzt, J., 2016. The pathogenesis of foot-and-mouth disease in pigs. Front. Vet. Sci. 3, 41.
Vidy, A., El Bougrini, J., Chelbi-Alix, M.K., Blondel, D., 2007. The nucleocytoplasmic rabies virus P protein counteracts interferon signaling by inhibiting both nuclear accumulation and DNA binding of STAT1. J. Virol. 81, 4255–4263.
Wang, C., Feng, H., Zhang, X., Li, K., Yang, F., Cao, W., Liu, H., Gao, L., Xue, Z., Liu, X., Zhu, Z., Zheng, H., 2021. Porcine picornavirus 3C protease degrades PRDX6 to impair PRDX6-mediated antiviral function. Virol. Sin. 36, 948–957.
Wang, D., Fang, L., Li, K., Zhong, H., Fan, J., Ouyang, C., Zhang, H., Duan, E., Luo, R., Zhang, Z., Liu, X., Chen, H., Xiao, S., 2012. Foot-and-mouth disease virus 3C protease cleaves NEMO to impair innate immune signaling. J. Virol. 86, 9311–9322.
Wang, D., Fang, L., Luo, R., Ye, R., Fang, Y., Xie, L., Chen, H., Xiao, S., 2010. Foot-and-mouth disease virus leader proteinase inhibits dsRNA-induced type I interferon transcription by decreasing interferon regulatory factor 3/7 in protein levels. Biochem. Biophys. Res. Commun. 399, 72–78.
Wu, X., Qi, J., Cong, X., Chen, L., Hu, Y., Yoo, D., Wang, G., Tian, F., Li, F., Sun, W., Chen, Z., Guo, L., Wu, J., Li, J., Wang, J., Zhao, X., Du, Y., 2018. Establishment and characterization of a high and stable porcine CD163-expressing MARC-145 cell line. BioMed Res. Int. 1–9, 2018.
Yokosawa, N., Kubota, T., Fujii, N., 1998. Poor induction of interferon-induced 2',5'-oligoadenylate synthetase (2-5 AS) in cells persistently infected with mumps virus is caused by decrease of STAT-1 alpha. Arch. Virol. 143, 1985–1992.
Young, D.F., Didcock, L., Goodbourn, S., Randall, R.E., 2000. Paramyxoviridae use distinct virus-specific mechanisms to circumvent the interferon response. Virology 269, 383–390.